A New Predictive Current Controller for a PMSM with consideration of calculation delay

H.T. Moon and M. J. Youn

Department of EECS in Korea Advanced Institute of Science and Technology

TaeJon, Korea

Abstract-- In a digital system, there are inevitable delays in calculations and applying the inverter output voltages to the motor terminals. Because of the delays, the conventional predictive current controller implemented in the digital system has large overshoot and large harmonics. A new predictive current controller, considering the delays, for a permanent magnet synchronous motor (PMSM) is presented. The effectiveness and feasibilities are shown by experimental results.

Keywords-- discrete time system, current control, and permanent magnet machines

I. INTRODUCTION

To implement the predictive current controller in the digital system, very high-speed calculation devices compared to the motor electrical dynamics are needed [1]. Otherwise, a modification is needed to endure the performance in the analog system [2], since there exist inevitable delays in calculations and applying the control output to the motor [3].

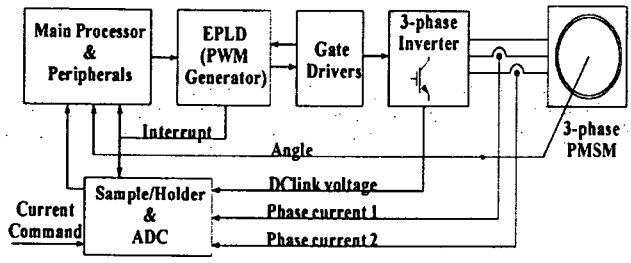

Fig. 1 Block diagram of the control system

Fig. 1 shows a simplified diagram of a typical PMSM servo drive system using digital processing devices. The control operation is synchronized with the interrupt signal generated by the pulse width modulation (PWM) generator. Usually two stator currents and a dc link voltage are sampled and held at the same time in an ADC and the rotor position is also sensed by the interrupt occurrence. The output values of the current controller are loaded on the PWM generator synchronized with the next interrupt signal. Switching signals are generated by the digital comparator in the PWM generator and are applied to a PWM inverter, which consists of six power switches. The phase voltages to drive the PMSM are fed by the constant voltage PWM inverter.

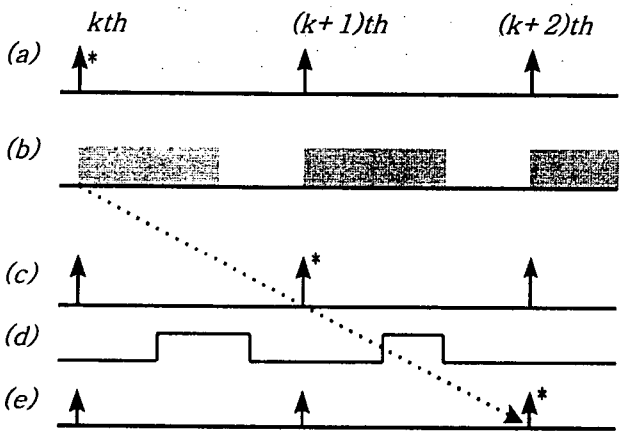

Fig. 2 Time sequence of the current control

Fig.2 shows the time sequence of the current controller. The *k*-th interrupt signal generated by the PWM generator starts the control process, as shown in Fig.2 (*a*). The gray part shown in Fig. 2 (*b*) is duration for calculating the current control and the blank is duration for conditional branches and down loading of the PWM values to the PWM generator. The output value of the current controller is uploaded to the PWM generator just before the (*k+1*)-th

interrupt signal shown in Fig. 2 (c). During the $(k+1)$-th period, the phase voltages calculated in the previous period are applied to the motor as shown in Fig. 2 (*d*). The resultant controlled currents are sensed, using the $(k+2)$-th interrupt signal, at the start of the $(k+2)$-th period of the current control process as shown in Fig. 2 (*e*). The controller needs one sampling period for calculation and the other period for applying the voltage to the motor. However, control process happens consecutively, the effective sampling period is one period. Due to the calculation delay, the conventional predictive current controller cannot be applied to the upper mentioned control system.

II. MODELING OF THE SYSTEM

A PMSM considering in this paper consists of permanent magnets mounted on the rotor surface and three phase stator windings are symmetrical, sinusoidally distributed and displaced by 120° in electrical degrees. The stator voltage equations of a PM synchronous motor in the synchronous reference frame are described as follows :

$$v_{qs} = R_s i_{qs} + L_s \cdot di_{qs}/dt + L_s \omega_r i_{ds} + \psi_m \omega_r \quad (1)$$

$$v_{ds} = R_s i_{ds} + L_s di_{ds}/dt - L_s \omega_r i_{qs} \quad (2)$$

where R_s is the stator phase resistance, L_s is the stator inductance, ω_r is the rotor angular velocity, ψ_m is the flux linkage established by the permanent magnet, and p is the number of rotor poles. The sampling period is short enough to assume the constant rotor speed. From (1) and (2), the discrete-time equation can be described as follows:

$$v_{qs}(k) = R_s i_{qs}(k) + \frac{L_s}{T_s} \cdot \left[i_{qs}(k+1) - i_{qs}(k) \right] + L_s \omega_r i_{ds}(k) + \psi_m \omega_r \quad (3)$$

$$v_{ds}(k) = R_s i_{ds}(k) + \frac{L_s}{T_s} \cdot \left[i_{ds}(k+1) - i_{ds}(k) \right] - L_s \omega_r i_{qs}(k) \quad (4)$$

where T_s is a sampling period. Using the nominal parameters, (3) and (4) can be rewritten as follows:

$$\mathbf{I}(k+1) = \mathbf{M} \cdot \mathbf{I}(k) + \mathbf{B} \cdot \mathbf{V}(k) + \mathbf{D} \cdot \Psi \quad (5)$$

where $\mathbf{I}(k) = \left[i_{qs}(k) \quad i_{ds}(k) \right]^T$, $\mathbf{V}(k) = \left[v_{qs}(k) \quad v_{ds}(k) \right]^T$,

$\Psi = \omega_r \left[\psi_m \quad 0 \right]^T$ $\mathbf{M} = \begin{bmatrix} 1 - T_s R_s / L_s & -T_s \omega_r \\ T_s \omega_r & 1 - T_s R_s / L_s \end{bmatrix}$,

$\mathbf{B} = T_s \begin{bmatrix} 1/L_s & 0 \\ 0 & 1/L_s \end{bmatrix}$, and $\mathbf{D} = -T_s \begin{bmatrix} 1/L_s & 0 \\ 0 & 1/L_s \end{bmatrix}$.

$i_{qs}(k)$ and $i_{ds}(k)$ are the dq transformed currents, and $v_{qs}(k)$ and $v_{ds}(k)$ are the dq transformed voltages, respectively. The rotor speed (ω_r) and magnetic flux (Ψ_m) can be considered as a constant in a control period.

III. THE CONVENTIONAL PREDICTIVE CURRENT CONTROLLER

In the conventional current controller, voltage commands of each axis are obtained from (3) and (4) or solve (5) for $\mathbf{V}(k)$ such as:

$$\mathbf{V}(k) = \mathbf{B}^{-1}(\mathbf{I}^*(k+1) - \mathbf{M} \cdot \mathbf{I}(k) - \mathbf{D} \cdot \Psi) \quad (6)$$

Most implementations in discrete system of the conventional predictive current controller, calculation time is short enough to consider infinitely small. For the case of it is hardly considered the calculation is infinitely small, however, various compensation methods are reported. The compensation methods have also overshoot in transient state [4].

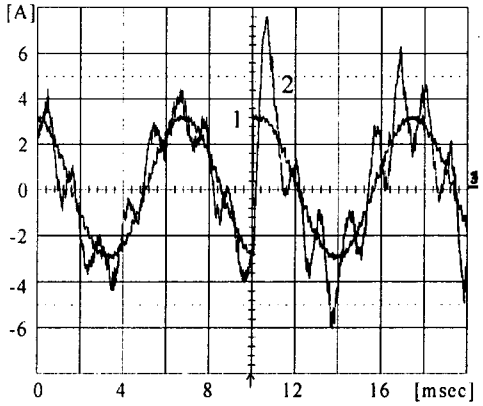

Fig. 3. Current response of the conventional predictive current controller implemented in discrete system.

Fig. 3 shows the control result of the conventional predictive current controller implemented in the upper mentioned discrete system. Trace 1 is the current command in a phase and trace 2 is the corresponding phase current. It shows large overshoot in transient state and large harmonics in steady state response.

IV. A NEW PREDICTIVE CURRENT CONTROLLER

During the (k+1)-th period, motor currents are excited by the control voltage $\mathbf{V}(k+1)$ which is calculated in the k-th period as shown in Fig. 2 (*d*). The resultant current can be expressed as follows:

$$\mathbf{I}(k+2)=\mathbf{M}\cdot\mathbf{I}(k+1)+\mathbf{B}\cdot\mathbf{V}(k+1)+\mathbf{D}\cdot\Psi. \quad (7)$$

It can be seen that the resultant current $\mathbf{I}(k+2)$ is affected by the states of $\mathbf{I}(k+1)$ and control voltage $\mathbf{V}(k+1)$. However, the voltage $\mathbf{V}(k+1)$ should be calculated using the information on currents and voltages of the k-th state. The relationship between the information on present k-th states and resultant current, $\mathbf{I}(k+2)$, can be described as follows:

$$\mathbf{I}(k+2)=\mathbf{M}\cdot\{\mathbf{M}\cdot\mathbf{I}(k)+\mathbf{B}\cdot\mathbf{V}(k)+\mathbf{D}\cdot\Psi\}$$
$$+\mathbf{B}\cdot\mathbf{V}(k+1)+\mathbf{D}\cdot\Psi. \quad (8)$$

For the regulation of the current, $\mathbf{I}(k+2)$ can be regarded as the desired current vector $\mathbf{I}^*$. Under the conditions of constant motor parameters and rotor speed during two sampling periods, the control output voltage $\mathbf{V}(k+1)$ which will be applied to the motor during the (k+1)-th period is described as follows:

$$\mathbf{V}(k+1)=\mathbf{B}^{-1}\{\mathbf{I}^*-\mathbf{M}\cdot\{\mathbf{M}\cdot\mathbf{I}(k)-\mathbf{B}\cdot\mathbf{V}(k)-\mathbf{D}\cdot\Psi\}+\mathbf{D}\cdot\Psi\}. \quad (9)$$

where $\mathbf{I}^*$ is the current command vector and $\mathbf{V}(k)$ is the present voltage vector applying to the motor during the k-th period. Under the conditions that $\mathbf{B}$ is inversable and $|\mathbf{V}(k)|$ is below the practical maximum voltage, $\mathbf{V}(k+1)$ can be obtained from the information on the present states. If the calculated voltage command is greater than the real voltage limitation, the real current can be reached to the current command when the following condition is satisfied:

$$\sum_{m=k_0+1}^{k_0+1+n}\Delta\mathbf{I}_{\max}(m)\geq\{\mathbf{I}^*-\mathbf{I}(k_0+1)\}. \quad (10)$$

where $\Delta\mathbf{I}_{\max}(m)$ is the maximum available current variation of the motor during the control period, k_0 is the instant when a new current command is given, and n is a positive integer.

V. IMPLEMENTATION AND EXPERIMENTAL RESULTS

A. Considerations in implementation

The sampling period (T_s) of the current control loop is 200 [μs]. The DC link voltage is 200 [V]. The ratings and parameter values of the PMSM are listed in Table 1.

Table. 1. Specifications of 750W PMSM

Rated power: 750W	**rated speed: 3000rpm**
***Rs*: 0.49Ω**	***Ls*: 6.9mH**
***Kt*: 0.4 Nm/Apeak**	**# of Poles: 8**

The PWM scheme in voltage source inverter is an important part of the current regulation for the PMSM. In this paper the space vector PWM is used to make phase voltages from the dq-axes voltages. It is well known that the space vector PWM is a preferable scheme for an instantaneous current controller because it gives a large linear control range, less harmonic distortion, and fast transient [5]-[7]. The voltage space vectors are corresponding to 8 switching states of the inverter. The lengths of voltage vectors corresponding to 6 active states are of length $V_{dc}2/3$ and these vectors form a hexagon. The voltage vectors u_0 and u_7 corresponding to the free-wheeling states are zero voltage vectors.

The corresponding reference voltage space vector V_s is calculated from the voltage commands $v^*_q(k+1)$, $v^*_d(k+1)$, the rotor angle θ_r, and the dc-link voltage. The relation between space voltage vector and the calculated command voltages is shown in Fig. 4. The on-durations for two

vector states are calculated by solving following equations [8]:

$$(t_a u_a + t_b u_b) = V_s \cdot T_s \quad (11a)$$

$$t_0 = T_s - t_a - t_b \quad (11b)$$

where u_a and u_b are the two switching state vectors adjacent in space to the reference vector V_s. The solutions of (11a) and (11b) are the on-durations t_a, t_b, and t_0 of the switching state vectors u_a, u_b, and u_0, respectively, and are expressed as follows:

$$t_a = 3 \cdot (\cos\theta - \sin\theta / \sqrt{3}) \cdot V_s \cdot T_s / (2 \cdot V_{dc}) \quad (12a)$$

$$t_b = \sqrt{3} \cdot V_s \cdot T_s \cdot \sin\theta / V_{dc} \quad (12b)$$

$$\theta = \theta_r - \gamma \quad (12c)$$

where V_{dc} is the dc-link voltage, V_s is the magnitude of the space vector V_s and the angle γ is $\tan^{-1}(v^*_d(k+1)/ v^*_q(k+1))$.

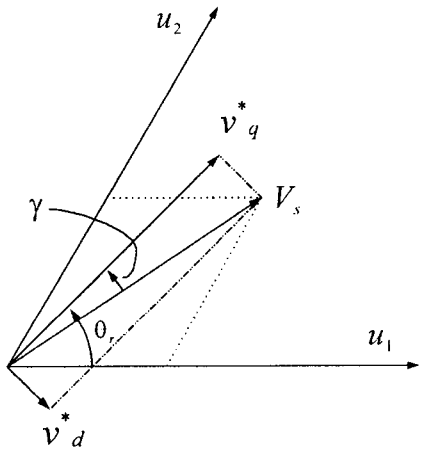

Fig. 4. Vector diagram of the relation between voltage commands and space voltage vector

If the magnitude of the space voltage vector is larger than the available output voltage, in this paper, the space vector is adjusted as follows:

$$v^{**}_q(k+1) = v^*_q(k+1) \frac{V_{dc}}{\sqrt{3} \cdot V_s} \quad (13a)$$

$$v^{**}_d(k+1) = v^*_d(k+1) \frac{V_{dc}}{\sqrt{3} \cdot V_s} \cdot \quad (13b)$$

where $v^{**}_q(k+1)$and $v^{**}_d(k+1)$ are rescaled control voltages.

B. Experimental results

Fig. 5 shows the current dynamics of the proposed predictive current controller. The rotor speed is about 1800 [rpm] and the q-axis current command is changed from 3[A] to -3[A] while the d-axis command is maintained at zero. In this figure, it is also observed that i_q reaches the steady state in 600 [μs] after the change of the current command.

Since the summation of the back EMF and required voltage for the current variation is larger than the voltage limitation, the real current cannot reach the reference current in a 2-sampling period, but in a 3-sampling period. If the operating speed is high and the change of the current command is large, it will take more periods until (10) is satisfied.

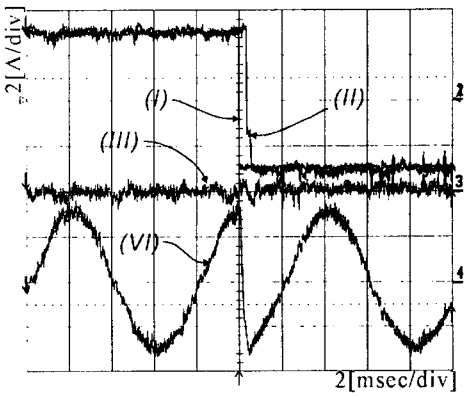

Fig. 5. Current dynamics of the proposed current controller. (I) is q- axis current command, (II) is q- axis measured current, (III) is d- axis measured current and (IV) is A phase current

Fig. 6. shows experimental results of the voltage limitations when the current command is changed sequentially from 3 [A], -3[A] and 3 [A] at a constant load condition. In Fig.6., trace 1 is the magnitude of the space voltage vector, trace 2 is the applied phase voltage, trace is the current command of a phase and trace 4 is the corresponding resultant current .

The speed of the rotor is changed in small variation during the changes of the current command so that the back EMF

is almost same. The difference between voltage commands in two cases is the voltage for the current variation. In a rising case, the motor is in powering mode, and the required voltage for the current variation is added to the back EMF and the total voltage is beyond the voltage limit.Until the phase current reaches the command value, the control voltage maintained the maximum voltage.

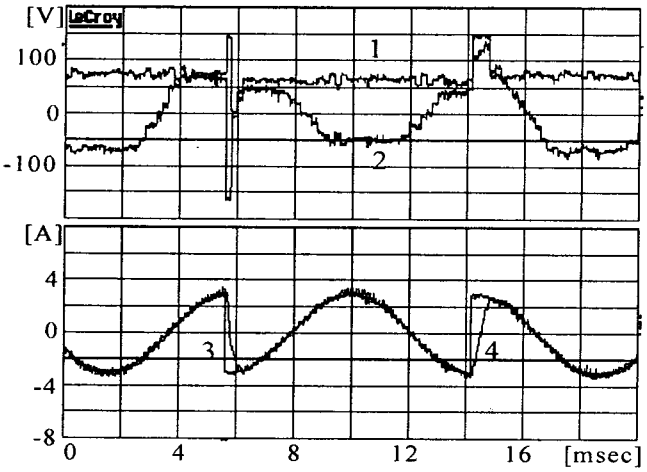

Fig. 6. Current command and corresponding voltage output of the controller

In a falling case, unlike the rising case, it is in generating mode, the voltage command is within the voltage limitation, since the part of the control voltage for the current variation is subtracted from the back EMF. As a result, it can be expected that the slope of the current variation depends upon the dc link voltage and operating conditions.

VI. CONCLUSIONS

This paper presents a new predictive current control method for a PMSM, considering the finite calculation delay of the control devices. The conventional predictive current controller is hard to implement in the fully digitized current controller for a small electrical constant PMSM, since the control period should be short enough and the calculation time is not infinitely small. Modifying the conventional predictive current controller to consider the calculation delay gives a large improvement in the current control performance in transient state and steady state. However, even with this improvement, the proposed current controller has limitation in real system since there exist voltage limitation. By considering the voltage limitation in the proposed current controller output dynamics is also expected.

Experimental results show that the performance of the proposed current controller is exceptional. After the analyzing and compensation of the voltage limitation, the performance of the proposed current controller is enhanced.

REFERENCES

[1] H. Lehuy, K. Slimani, , and P. Viarouge, "Analysis and Implementation of a Real-time Predictive Current Controller for Permanent-Magnet Synchronous Servo Drives," *IEEE Trans. Ind. Elect.*, vol. 41, no. 1, pp. 110-117, 1994

[2] D. G. Holmes, and D. A. Martin, "Implementation of a direct digital predictive current controller for single and three phase voltage source inverters," *Industry Applications Conference*, pp. 906 –913, 1996.

[3] J. Haylock, B. Mecrow, A. Jack, and D. Atkinson, "Enhanced current control of high-speed PM machine drives through the use of flux controllers," *IEEE Trans. Ind. Applicat.* Vol. 35, no. 5, pp. 1030-1038, 1999.

[4] O. Kukrer, " Discrete-time current control of voltage-fed three-phase PWM inverter," *IEEE Trans. Power Electron.*, vol. 11, no.2, pp. 260-269, March 1996.

[5] J. Holts, "Pulsewidth modulation for electronic power conversion," *Proc. IEEE*, vol. 82, no. 8, pp. 1194-1214, August 1994.

[6] J. Holts, "Pulsewidth modulation --- a survey," *IEEE Trans. Ind. Elect.*, vol. 39, no. 39, pp. 410-420, Dec. 1992.

[7] J. Richardson and O. T. Kukrer, "Implementation of a PWM regular sampling strategy for AC drives," *IEEE Trans. Power Electron.*, vol. 6, no.4, pp. 645-655, October 1991.

[8] H. W. Vander Broeck, H. C. Skudelny, and G. V. Stanke, "Analysis and realization of a pulsewidth modulator based on voltage space vectors," *IEEE. Trans. Ind. Applicat.*, vol. 24, no.1, pp. 142-150, Jan./Feb. 1988.